Electronic Supplementary Material (ESI) for Lab on a Chip.
This journal is © The Royal Society of Chemistry 2022

Direct MYD88^{L265P} gene detection for diffuse large B-cell lymphoma (DLBCL) *via* a miniaturised CRISPR/dCas9-based sensing chip

Weihan Sun[1,2,†], Wei Guo[4,†], Zhiyi Liu[2], Sennan Qiao[1], Ziming Wang[1], Jiayu Wang[2], Lingxuan Qu[2], Liang Shan[1], Fei Sun[1,2,*], Shuping Xu[3,*], Ou Bai[4,*], Chongyang Liang[1,2,*]

[1] Department of Biopharmacy, School of Pharmaceutical Sciences, Jilin University, 1266 Fujin Road, 130021 Changchun, China.

[2] Institute of Frontier Medical Science, Jilin University, 1163 Xinmin Street. 130021 Changchun, China.

[3] State Key Laboratory of Supramolecular Structure and Materials, Institute of Theoretical Chemistry, College of Chemistry, Jilin University, 2699 Qianjin Ave. 130012 Changchun, China.

[4] Department of Hematology, The First Hospital of Jilin University, Jilin University, 71 Xinmin Street. 130021 Changchun, China.

†These authors contributed equally to this article

*Correspondence: **Chongyang Liang**(liang@jlu.edu.cn); **Fei Sun** (sunfei@jlu.edu.cn); **Shuping Xu** (xusp@jlu.edu.cn); **Ou Bai** (baiou@jlu.edu.cn)

Supplementary Material

The pColdIV/dCas9 expression vector (plasmid expressing S. pyogenes Cas9 protein with mutations of RuvC and HNH catalytic residues) was purchased from GenScript (GenScript, NJ). dCas9 proteins were obtained from Escherichia coli BL21 in our laboratory and amplified by fermentation in 7.5-L fermenter (BIOFLO II-New Brunswick) and purified by AKTA (GE Healthcare). sgRNA sequences were synthesized using HiScribe T7 High Yield RNA Synthesis Kit (NEB) following the Standard RNA Synthesis protocol. Primer sequences designed by Primer 5 and synthesized by GenScript (GenScript, NJ). Whole-genome DNA (gDNA) were extracted by Blood/Cell/Tissue Genomic DNA Extraction Kit from TIANGEN® according to the manufacturer's protocol. The extracted gDNA was measured by using NanoDrop 2000 UV-vis spectrometer (Thermo Fisher Scientific, DE, USA) to confirm its concentration. The gDNA was diluted to proper concentration and stored at -80 ˚C before use. Other chemicals were obtained from Sigma Aldrich (USA). The qPCR was performed using the Analytic Jena Q-tower system (Analytik-Jena, Jena, Germany). PAA chips were produced by our laboratory. Electrical measurements were conducted using a Keithley 2450 (Keithley Instruments), and the ZLD type plasma airsickness was used for the the hydroxylation modification of the PAA membrane surface.

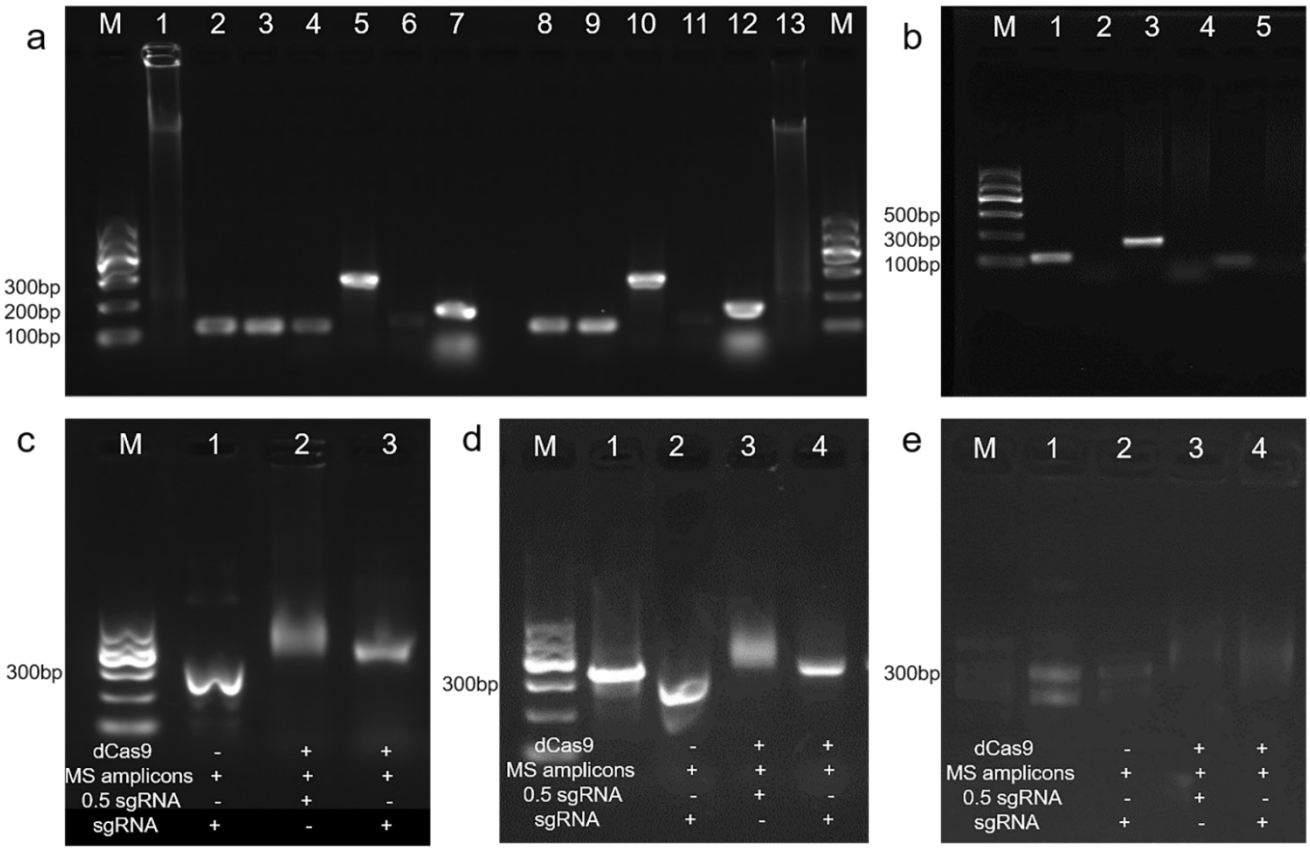

Figure S1. Electrophoresis images of MYD88^{L265P} site-specificity and sgRNA activity detection. (a)Electrophoretic bands correspond to: lane1: M1 original full genome sequence, lane 2/3: MC primers were used to target M1 PCR products, lane 4: WC primers were used to target M1 PCR products, lane 5: MS primers were used to target M1 PCR products, lane 6: WS primers were used to target M1 PCR products, lane 7: M primers were used to target M1 PCR products, lane 8: MC primers were used to target M2 PCR products, lane 9: WC primers were used to target M2 PCR products, lane 10: MS primers were used to target M2 PCR products, lane 11: WS primers were used to target M2 PCR products, lane 12: WM primers were used to target M2 PCR products, lane 13: M2 full genome sequence. (b) Electrophoretic bands correspond to: lane 1: MC primers were used to target M3 PCR products, lane 2: WC primers were used to target M3 PCR products, lane 3: MS primers were used to target M3 PCR products, lane 4: WS primers were used to target M3 PCR products, lane 5: M primers were used to target M3 PCR products. (c) Binding activity test results of M1 positive patient. The strips correspond to Table 2, respectively. (d) and (e) correspond to the M2 and M3 positive patients, respectively.

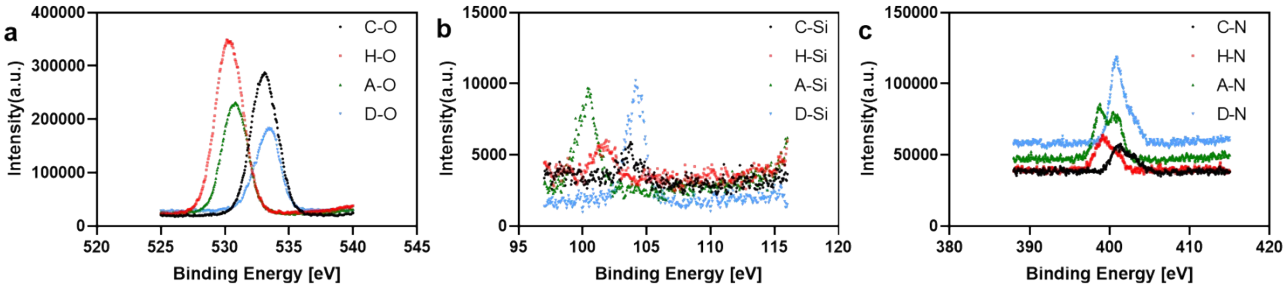

Figure S2. For the unmodified blank chip (black line), the hydroxylated chip (red line), the chip after adding APTES reaction (green line), and the PAA chip after dehydration and cross-linking in the amination (blue line) to detect the intensity changes of (a) oxygen, (b) silicon, and (c) nitrogen.

Four element intensity changes were detected for PAA under the following states: the blank chip without modification (C), the chip after hydroxylation (H), the chip after adding APTES reaction (A), and the chip after dehydration and cross-linking in amination state (D). The hydroxyl oxygen is around 531 eV can be used as the X-axis reference. After hydroxylation modification, the intensity of the oxygen element increases significantly, and the following two steps of modification result in a decrease of the strength of the oxygen element, as shown in Fig. S2a, indicating that the hydroxylation modification is successful. Compared with the blank chip, the silicon after adding APTES reaction and amination modification is significantly improved (Fig. S2b). The corresponding X axis of nitrogen element is 398 eV. Compared with other steps, the chip strength of amination after dehydration and cross-linking is significantly increased (Fig. S2c). The signal of high nitrogen element was detected, indicating that the hydroxylation and amination modifications were noticeable.

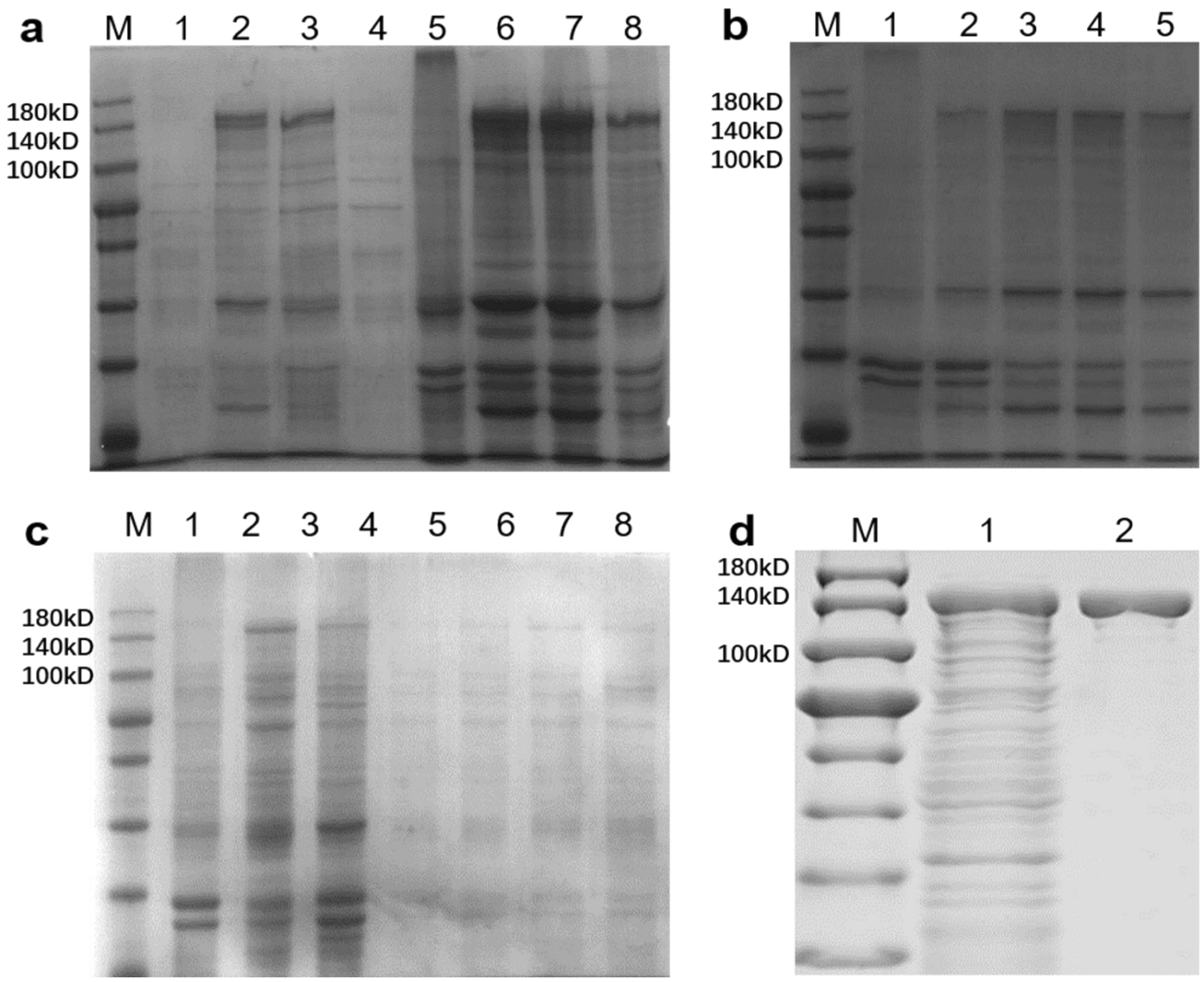

Figure S3. SDS-PAGE detection results correspond to dCas9 protein expression, fermentation, and purification. (a) The temperature gradient was set to optimize the expression, and the bands represented: lane 1: Negative control supernatant, lane 2: 16℃ induced supernatant, lane 3: 25℃ induced supernatant, lane 4: 37℃ induced supernatant, lane 5: Negative control precipitation, lane 6: 16℃ induced precipitation, lane 7: 25℃ induced precipitation, lane 8: 37℃ induced precipitation. (b) Screening IPTG concentration gradient. lane 1: Negative control precipitation, lane 2: 0.1mM IPTG, lane 3: 0.5mM IPTG, lane 4: 1.0mM IPTG, lane 5: 2.0mM IPTG. (c) Optimization of bacterial density (OD600). lane 1: Negative control supernatant, lane 2: OD≈0.4 supernatant, lane 3: OD≈0.6 supernatant, lane 4: OD≈1.0 supernatant, lane 5: Negative control precipitation, lane 6: OD≈0.4 precipitation, lane 7: OD≈0.6 precipitation, lane 8: OD≈1.0 precipitation. (d) lane 1: Sample after fermentation in fermenter, lane 2: The sample was purified by affinity chromatography.

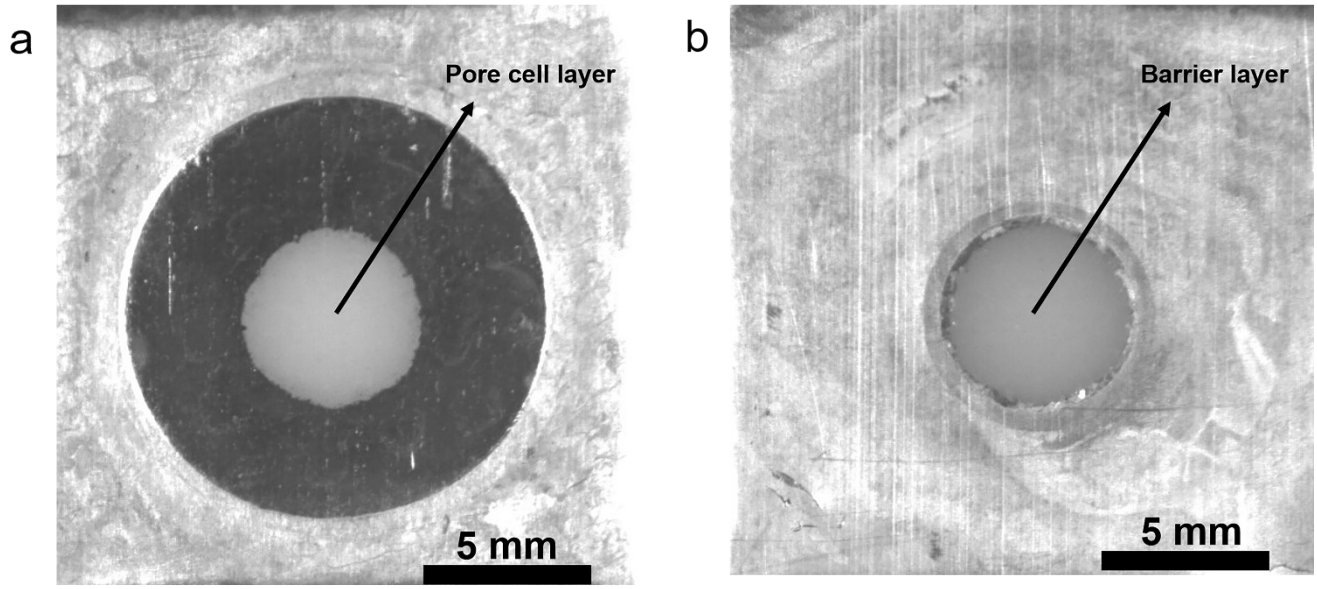

Figure S4. The optical photograph of (a) the PAA with a pore cell layer. (b) The PAA with a barrier layer. The thickness of the diaphragm is between 40 and 70 nm and the diameter is 5 mm. The scale bars are 5 mm.

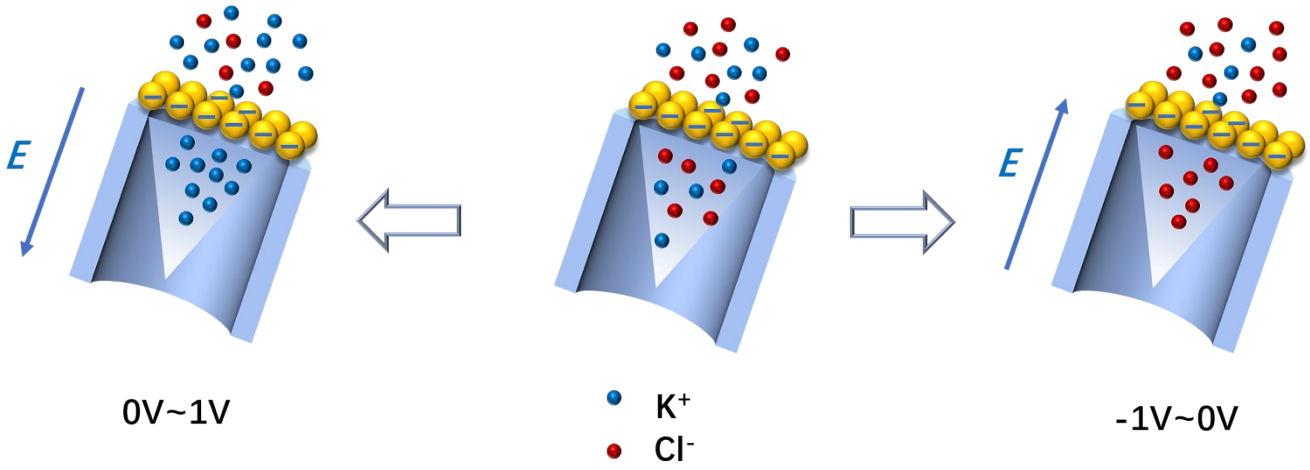

Figure S5. Schematic diagram of the passage about K+ and Cl- through PAA under different voltage ranges.

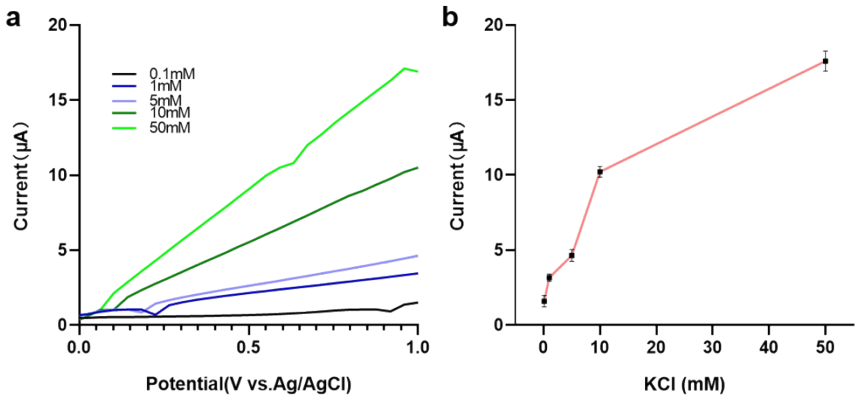

Figure S6. Screening results of KCl electrode buffer concentration. (a) I−V curves of different KCl concentrations worked on bare PAA. (b) Detection charts of three parallel groups were set for each KCl concentration.

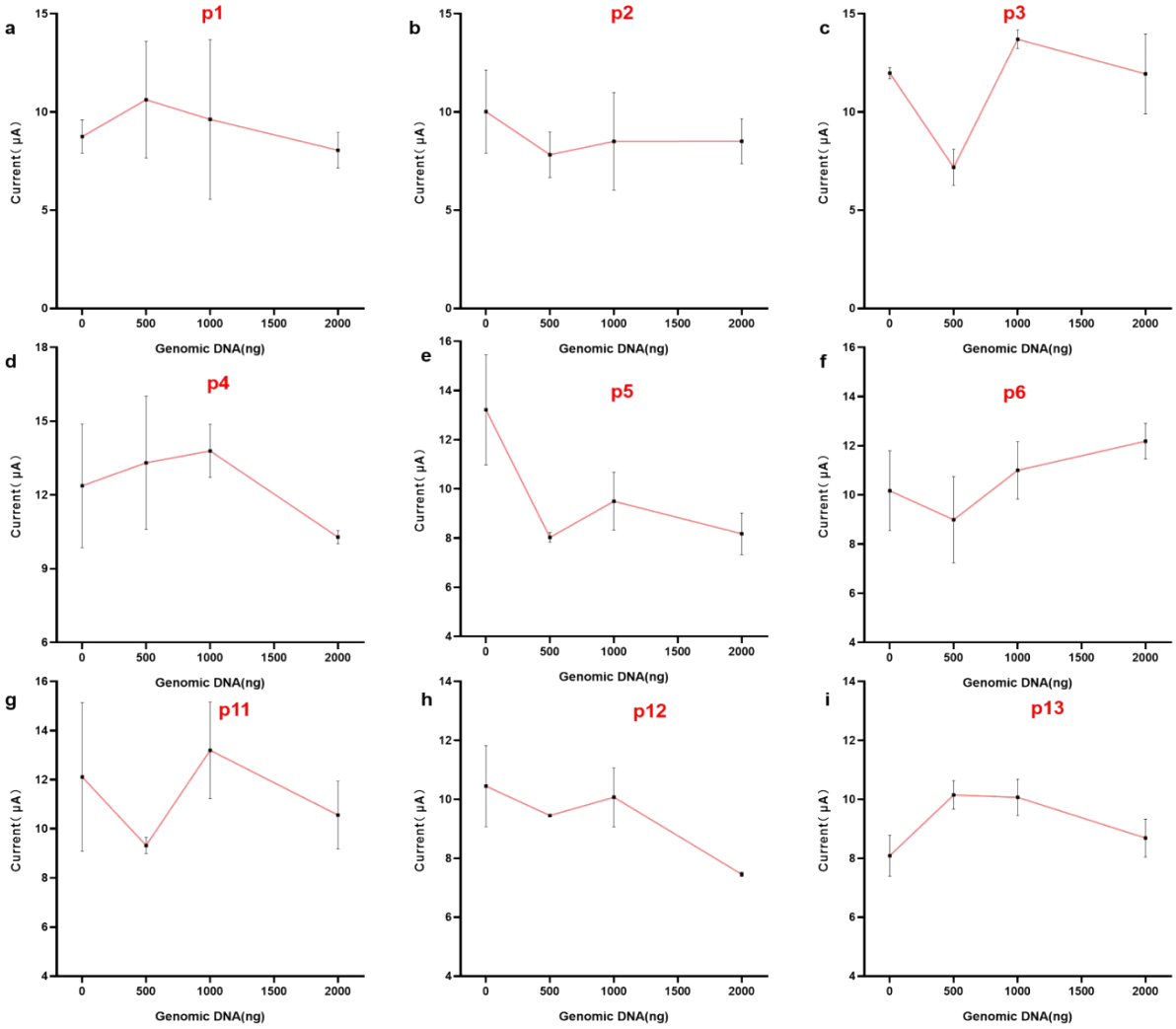

Figure S7. The intensity curves of the CRISPR–PAA sensing chip for the remaining 9 clinical patient samples. (a) The intensity curves of the parallel samples of P1(No 1 Patient), under the condition of +1.0 V. (b)-(i) The intensity curves of the parallel samples of P2-P6 and P11-P13, respectively, under the condition of +1.0 V.

Table S1. Primer sequences for MYD88^{L265P}

Description	Name	Sequence (5'to 3')
Wild-type primers	WC-F	CATCAGAAGCGACTGATCCC
	WM-F	CCCATCAGAAGCGACTGATC
	WS-R	CTTGATGGGGATCGGTCGCTT
Mutant primers	MC-F	CATCAGAAGCGACCGATCCC
	MM-F	CCCATCAGAAGCGACCGATC
	MS-F	GTAGGTGGGGCCTCTGGATT
	M-R	AAGGCGAGTCCAGAACCAAG
Universal primer	MYD88-F	AACCCTGGGGTTGAAGACTG
	MYD88-R	AGTCTTCAGGGCAGGGACAA

Table S2. dCas9 protein, sgRNA and template DNA binding reaction system.

Name	1	2	3
dCas9	0 μg	0.5 μg	0.5 μg
sgRNA	0.5 μL	0.5μL	1 μL
gDNA	1 μg	1 μg	1 μg
10×PBS Buffer	2 μL	2 μL	2 μL
RNase free H_2O	to 20 μL	to 20 μL	to 20 μL

Table S3. Clinical information of 13 patients and corresponding MYD88 mutation detection results.

Number	Resection site	Resection time	Pathological diagnosis	$MYD88^{L265P}$	Current (μA)
P1	Right axillary lymph node	Before treatment	Reactive hyperplasia of lymph node follicles	None	12.4996
P2	Inguinal lymph nodes	Before treatment	Angioimmunoblastic T cell lymphoma (AITL)	None	10.2627
P3	Left cervical lymph node	Before treatment	Diffuse large B cell lymphoma (DLBCL)	Negative	14.0392
P4	Left cervical lymph node	After relapse	B small cell lymphoma	None	13.0201
P5	Right submandibular lymph node	Before treatment	Lymphopapillary cystic tumor (Warthin tumor)	None	10.3330
P6	Left axillary lymph node	Before treatment	Diffuse large B cell lymphoma (DLBCL)	Negative	11.8325
P7(M1)	Left cervical lymph node	Before treatment	Diffuse large B cell lymphoma (DLBCL)	Positive	37.308
P8(M2)	Left cervical lymph node	Before treatment	Diffuse large B cell lymphoma (DLBCL)	Positive	33.3
P9(WT)	Left cervical lymph node	Before treatment	Diffuse large B cell lymphoma (DLBCL)	Negative	10.2
P10(M3)	Left inguinal lymph node	Before treatment	Diffuse large B cell lymphoma (DLBCL)	Positive	34.985
P11	Right inguinal lymph node	After relapse	Lymph node marginal zone lymphoma （NMZL）	None	11.8094
P12	Left cervical lymph node	Before treatment	Granulomatous lymph node lesions	None	10.7836
P13	Left cervical lymph node	After relapse	Classic Hodgkin's Lymphoma-Nodular Sclerosis Type	None	10.5045